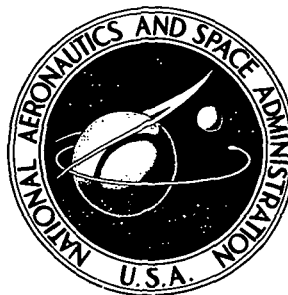


NASA TECHNICAL NOTE



NASA TN D-6991

NASA TN D-6991

CASE FILE  
COPY

CALIBRATION OF RADIATION DETECTORS  
IN THE ULTRAVIOLET REGION  
BETWEEN 972 AND 2500 Å

*by James O. McClenahan*

*Ames Research Center*

*Moffett Field, Calif. 94035*

NATIONAL AERONAUTICS AND SPACE ADMINISTRATION • WASHINGTON, D. C. • SEPTEMBER 1972

|   |   |   |                             |
|---|---|---|-----------------------------|
| 1. Report No.<br><b>NASA TN D-6991</b>  | 2. Government Accession No.                                 | 3. Recipient's Catalog No.  |                             |
| 4. Title and Subtitle<br><b>CALIBRATION OF RADIATION DETECTORS IN THE<br/>ULTRAVIOLET REGION BETWEEN 972 AND 2500 Å</b>   |   | 5. Report Date<br><b>September 1972</b>                           |                             |
|   |   | 6. Performing Organization Code                                   |                             |
| 7. Author(s)<br><b>James O. McClenahan</b>  |   | 8. Performing Organization Report No.<br><b>A-4456</b>            |                             |
|   |   | 10. Work Unit No.<br><b>117-07-04-11-00-21</b>                    |                             |
| 9. Performing Organization Name and Address<br><b>NASA Ames Research Center<br/>Moffett Field, Calif., 94035</b>  |   | 11. Contract or Grant No.   |                             |
|   |   | 13. Type of Report and Period Covered<br><b>Technical Note</b>    |                             |
| 12. Sponsoring Agency Name and Address<br><b>National Aeronautics and Space Administration<br/>Washington, D. C. 20546</b>  |   | 14. Sponsoring Agency Code  |                             |
|   |   | 15. Supplementary Notes   |                             |
| 16. Abstract<br><br><p>This report describes the development of experimental setups and procedures for calibrating photosensitive devices in the spectral range 1022 to 2500 Å for which no direct calibration techniques exist. An indirect technique that uses a sodium salicylate detector calibrated outside this range was developed for use as a secondary standard. The primary standard was a xenon-filled ionization chamber, which is an absolute standard over the wavelength interval 972 to 1022 Å. Measurements made by this method were checked at 1470 Å with a xenon lamp and at 2537 Å with a mercury arc lamp and a 0.5 m blaze monochromator with a grating blazed at 2000 Å. The overall accuracy of the measurements was ±40 percent or better.</p> |   |   |                             |
| 17. Key Words (Suggested by Author(s))<br><br><b>Calibration<br/>Ultraviolet<br/>Photomultiplier</b>  |   | 18. Distribution Statement<br><br><b>Unclassified – Unlimited</b> |                             |
| 19. Security Classif. (of this report)<br><b>Unclassified</b>   | 20. Security Classif. (of this page)<br><b>Unclassified</b> | 21. No. of Pages<br><b>15</b>                                     | 22. Price*<br><b>\$3.00</b> |

**CALIBRATION OF RADIATION DETECTORS**  
**IN THE ULTRAVIOLET REGION**  
**BETWEEN 972 AND 2500 Å**

James O. McClenahan

Ames Research Center

**SUMMARY**

This report describes the development of experimental setups and procedures for calibrating photosensitive devices in the spectral range 1022 to 2500 Å for which no direct calibration techniques exist. An indirect technique that uses a sodium salicylate detector calibrated outside this range was developed for use as a secondary standard. The primary standard was a xenon-filled ionization chamber, which is an absolute standard over the wavelength interval 972 to 1022 Å. Measurements made by this method were checked at 1470 Å with a xenon lamp and at 2537 Å with a mercury arc lamp and a 0.5 m blaze monochromator with a grating blazed at 2000 Å. The overall accuracy of the measurements was  $\pm 40$  percent or better.

**INTRODUCTION**

The shock layer produced by a vehicle entering the earth's atmosphere from a superorbital mission radiates strongly in the region between 1000 and 3000 Å. Absolute measurements of such radiation require the calibration of photosensitive devices, which is not possible over this entire region by direct methods.

For wavelengths greater than 2500 Å the calibration of photosensitive devices is possible because metals have stable properties at the temperatures required to produce such radiation; and excellent metal ribbon or filament lamps are available for accurately simulating black-body continua. For wavelengths below 1000 Å calibration schemes may be devised which use various gases that are ionized by photons in this spectral region. For wavelengths between 1022 and 2500 Å, however, there are no standard lamps or detectors for direct calibration. A secondary standard that uses sodium salicylate was therefore produced to bridge the interval between 1022 and 2537 Å.

The purpose of the work described here was to develop apparatus and procedures for calibrating photomultipliers in the wavelength range from 1040 to 2537 Å. General purpose laboratory equipment was used wherever possible so that the system would be flexible and could be modified with a minimum of effort. The aim of the work was first to calibrate a solar blind photomultiplier tube for use in a shock tube experiment and, second, to establish a systematic calibration procedure and describe it with sufficient detail to help others performing measurements in this region. Heavy reliance was placed on reference 1 in which the properties of many types of detectors and sources are discussed.

## EXPERIMENTAL PROCEDURE

Three different experimental procedures were used to establish the calibration curve of a solar blind photomultiplier tube between 1040 and 2537 Å. These procedures involved (1) calibration in the wavelength region  $1100 < \lambda < 1600$  Å using a sodium salicylate secondary standard, (2) calibration at 2537 Å using a mercury lamp, and (3) calibration at 1470 Å using a xenon-filled discharge lamp.

### Calibration at $1100 \text{ Å} < \lambda < 1600 \text{ Å}$

Calibration of the solar blind photomultiplier tube in the wavelength region  $1100 \text{ Å} < \lambda < 1600 \text{ Å}$  involved two steps: First, a sodium salicylate-coated photomultiplier tube was calibrated between 972 and 1022 Å as a secondary standard (using the ionization gage as a primary standard). Next, this secondary standard was used to calibrate the solar blind photomultiplier tube between 1100 and 1600 Å.

The experimental apparatus for this calibration is shown schematically in figure 1. The source of radiation was a Hinteregger type capillary tube discharge lamp (ref. 2) employing hydrogen. Typically, this lamp was operated at a discharge current of 0.4 A and a pressure of 4 Torr measured immediately upstream of the gas inlet to the lamp. A differential pumping station separated the

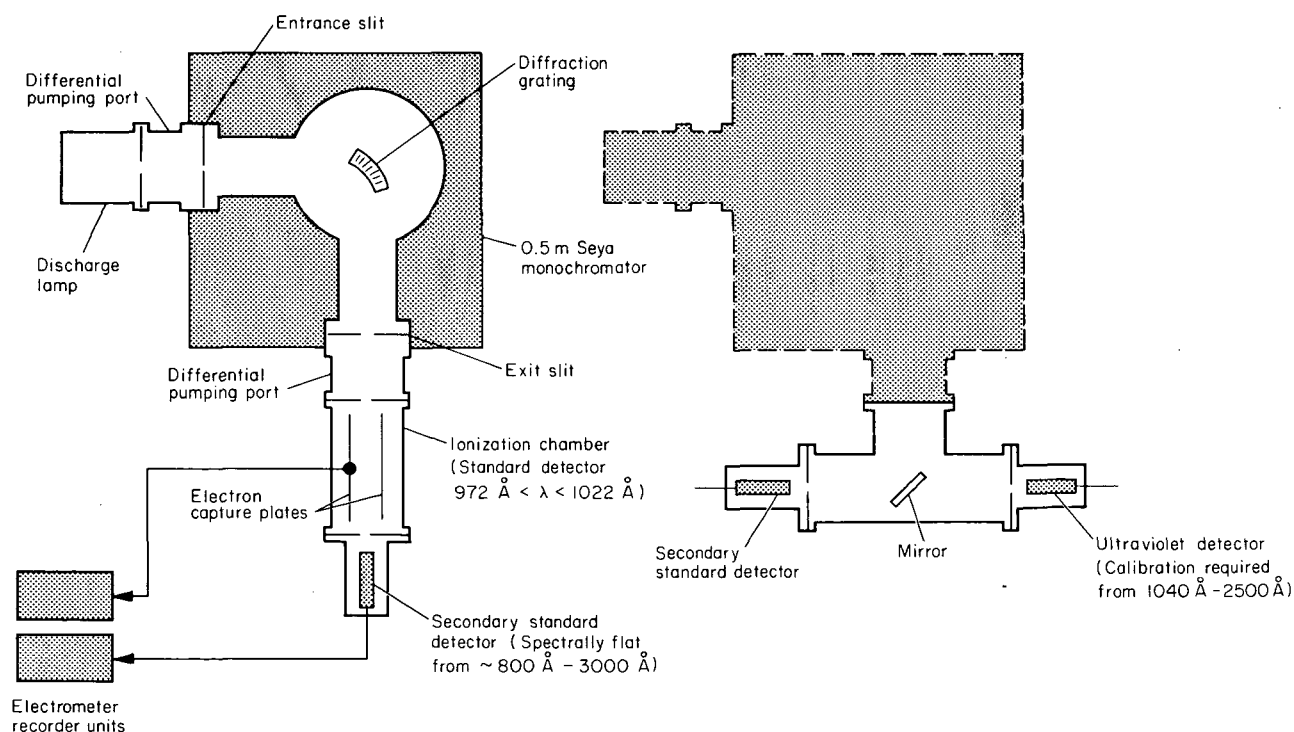


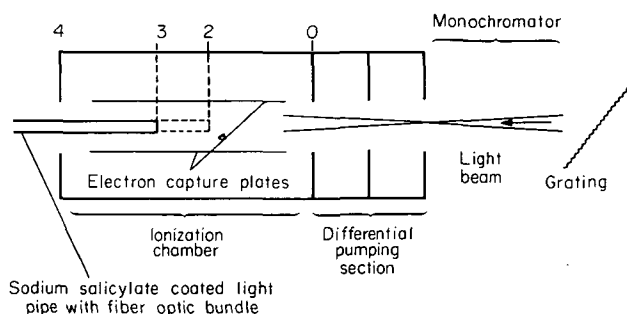
Figure 1. — Ultraviolet detector calibration setup.

lamp from monochromator, which was a 0.5 m Seya-Namioka type vacuum-ultraviolet monochromator (see ref. 3) with a 1200 line/mm grating blazed at 800 Å. The differential pumping station (see ref. 4) prevented an appreciable amount of gas from the source from flowing into the monochromator and thereby decreasing through absorption the light intensity available at the exit slit of the monochromator. A xenon-filled ionization chamber was the primary standard detector for these tests. In the wavelength region  $972 < \lambda < 1022$  Å, xenon has a photoionization quantum yield of unity (i.e., one electron is produced per photon absorbed; see ref. 5). Thus a properly constructed ionization chamber filled with xenon becomes an absolute standard in this wavelength region. Details of the construction and use of ionization chambers, typical of that used in this work, are presented in reference 6.

Calibration of the secondary standard involves (1) determination of the absorption coefficient of the gas in the ionization chamber, and (2) determination of the anode sensitivity of the sodium-salicylate secondary standard.

*Determination of the absorption coefficient*

The experimental setup for determining the absorption coefficient of the xenon gas used in the ionization chamber is shown in sketch (a). In this setup, the ionization chamber is used solely as a container for the xenon. A small moveable light pipe was used to measure the flux at two positions within the ionization chamber. The light pipe was a short length of glass tubing with its tip sealed by a sodium salicylate-coated flat disk. The visible light signal produced by fluorescence of the coating, due to ultraviolet radiation, was transmitted to the photomultiplier tube in a fiber optic bundle. If Beer's law holds within the absorption chamber, the output current of the photomultiplier tube is



Sketch (a)

$$i_j = k_j \gamma Q_0 \exp(-p\mu X_j) \quad (1)$$

where

$i_j$  output current of photomultiplier for position  $j$ , A

$\gamma$  anode sensitivity of photomultiplier, A/W

$k_j$  factor of proportionality that accounts for geometrical effects (i.e., not capturing all of the light that enters the ionization chamber).

$Q_0$  flux entering the ionization chamber at pressure  $p$ , W

$p$  pressure in the ionization chamber, Torr

$\mu$  absorption coefficient of the gas in the ionization chamber, Torr<sup>-1</sup> cm<sup>-1</sup>

$X_j$  distance from ionization chamber entrance to the front of the light pipe for  $j$ th position, m

If measurements are made at two locations in the ionization chamber (stations 2 and 3), the ratio of the photomultiplier tube currents is

$$\frac{i_3}{i_2} = \frac{k_3}{k_2} \exp[-p\mu(X_3 - X_2)] \quad (2)$$

As the pressure in the ionization chamber goes to zero, the flux entering the chamber goes to a maximum and

$$\frac{i_{3m}}{i_{2m}} = \frac{k_3}{k_2} \quad (3)$$

Combining equations (2) and (3) and solving for  $\mu$  gives

$$\mu = \frac{1}{p(X_3 - X_2)} \ln\left(\frac{i_3}{i_{3m}}\right)\left(\frac{i_{2m}}{i_2}\right) \quad (4)$$

The absorption coefficient was determined for several pressures and locations and was found to have a constant value of 0.0786 (Torr  $\text{cm}^{-1}$ ) to within a few percent. Constancy of this value is verification of the application of Beer's law within the ionization chamber for the range of pressures at which the calibration was performed.

Although a very efficient differential pumping system was used, some gas in both the differential pumping system and the monochromator remained in the lightpath and absorbed radiation. This absorption was a function of the gas pressure in the ionization chamber. With the ionization chamber filled to a given pressure  $p$  (within the Beer's law region), and the detector a distance  $X$  from the ionization chamber entrance slit, the flux entering the ionization chamber may be determined by use of equation (1):

$$Q_0 = Q_{0m} \frac{i_p}{i_m} \exp(p\mu x) \quad (5)$$

where

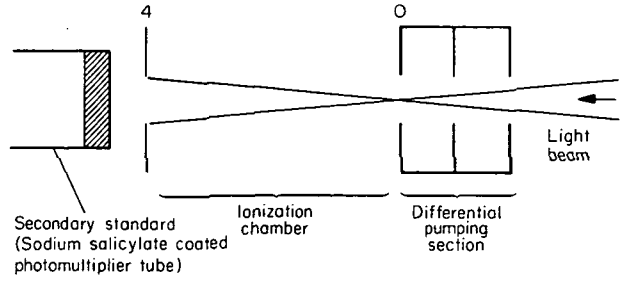
$Q_0$  flux entering the ionization chamber, W

$Q_{0m}$  flux entering the ionization chamber at pressure  $p = 0$ , W

$i_p$  output current of photomultiplier tube at pressure  $p$ , A

$i_m$  output current of photomultiplier tube at  $p = 0$ , A

**Determination of anode sensitivity of secondary standard**— The experimental set-up for determining the anode sensitivity of the secondary standard is shown in sketch (b). Several approaches can be used to determine the anode sensitivity of the secondary standard. The one used here relies on using the ionization chamber as an absolute standard combined with a pre-determined knowledge of the absorption coefficient of the gas in the ionization chamber. The output current of the secondary standard is



Sketch (b)

$$i_4 = K_{SS}Q_4 \quad (6)$$

where

$K_{SS}$  anode sensitivity of secondary standard, A/W

$Q_4$  flux falling on secondary standard, W

Care was taken in the experimental setup to ensure that the secondary standard viewed the entire solid angle of radiation that entered the ionization chamber. With this provision, the flux falling on the secondary standard is

$$Q_4 = Q_0 - Q_1 \quad (7)$$

where  $Q_1$  is the flux absorbed in the ionization chamber. Beer's law can be used to find the flux leaving the ionization chamber

$$Q_4 = Q_0 \exp(-p\mu\ell) \quad (8)$$

where  $\ell$  is the length of the ionization chamber. Combining equations (7) and (8) gives

$$Q_4 = \frac{Q_1}{\exp(p\mu\ell) - 1} \quad (9)$$

It should be noted here that the flux exiting the ionization chamber may be found without calculating the flux entering the chamber (eq. (5)). Substituting equation 9 into equation 6 and solving for  $K_{SS}$  gives

$$K_{SS} = \frac{i_4 [\exp(p\mu\ell) - 1]}{Q_1} \quad (10)$$

The output current of the photoionization chamber is given by

$$i_1 = K_{IC}Q_1 \quad (11)$$

with

$$K_{IC} = \frac{\gamma \lambda e}{hc} \quad (12)$$

where

$\gamma$  quantum efficiency of the gas in the ionization chamber, electron/photon ( $\gamma = 1$  for  $972 > \lambda > 1022 \text{ \AA}$ )

$\lambda$  wavelength of radiation entering the ionization chamber,  $\text{\AA}$

$e$  electron charge, C

$h$  Planck's constant, J-sec

$c$  speed of light,  $\text{\AA}/\text{sec}$

Finally, the anode sensitivity for the secondary standard can be written

$$K_{SS} = \frac{K_{IC} i_4 [\exp(p\mu\ell) - 1]}{i_1} \quad (13)$$

This sensitivity was determined at various wavelengths between 972 and 1022  $\text{\AA}$  (autoionization region for xenon) and was found to be constant to within  $\pm 10$  percent. Since sodium salicylate has a nearly constant quantum yield (see ref. 7), this sensitivity was used in the wavelength range  $1100 \text{ \AA} < \lambda < 1600 \text{ \AA}$ .

*Calibration of solar blind photomultiplier tube*— The experimental setup for calibrating the solar blind photomultiplier tube over the wavelength range  $1100 \text{ \AA} < \lambda < 1600 \text{ \AA}$  is shown in figure 1. In principle, the technique involved installing a tee at the output slit of the monochromator, and diverting the radiative flux to either the secondary standard or the solar blind photomultiplier tube by means of a rotatable front surface mirror. Care was taken to ensure that both detectors viewed the same solid angle, and the calibration was repeated at several wavelengths given by the hydrogen lamp (see ref. 8). The actual radiation spectrum obtained in this experiment as measured with the secondary standard is shown in figure 2.

#### Calibration at $\lambda = 2537 \text{ \AA}$

Solar blind photomultiplier tubes have long wavelength cutoffs defined by the natural response of the photocathode material. For the particular tube calibrated in this study, the cutoff was nominally 2500  $\text{\AA}$ . A cutoff in this region was required for this particular experiment. The use of a sodium salicylate detector system was precluded because the spectral sensitivity of such a system extends into the visible. The cutoff was not well defined by the manufacturer and since it is important that the system sensitivity be low above cutoff a separate calibration was made at  $\lambda = 2537 \text{ \AA}$ . The apparatus used is shown in figure 3. A mercury-arc lamp was used as the light



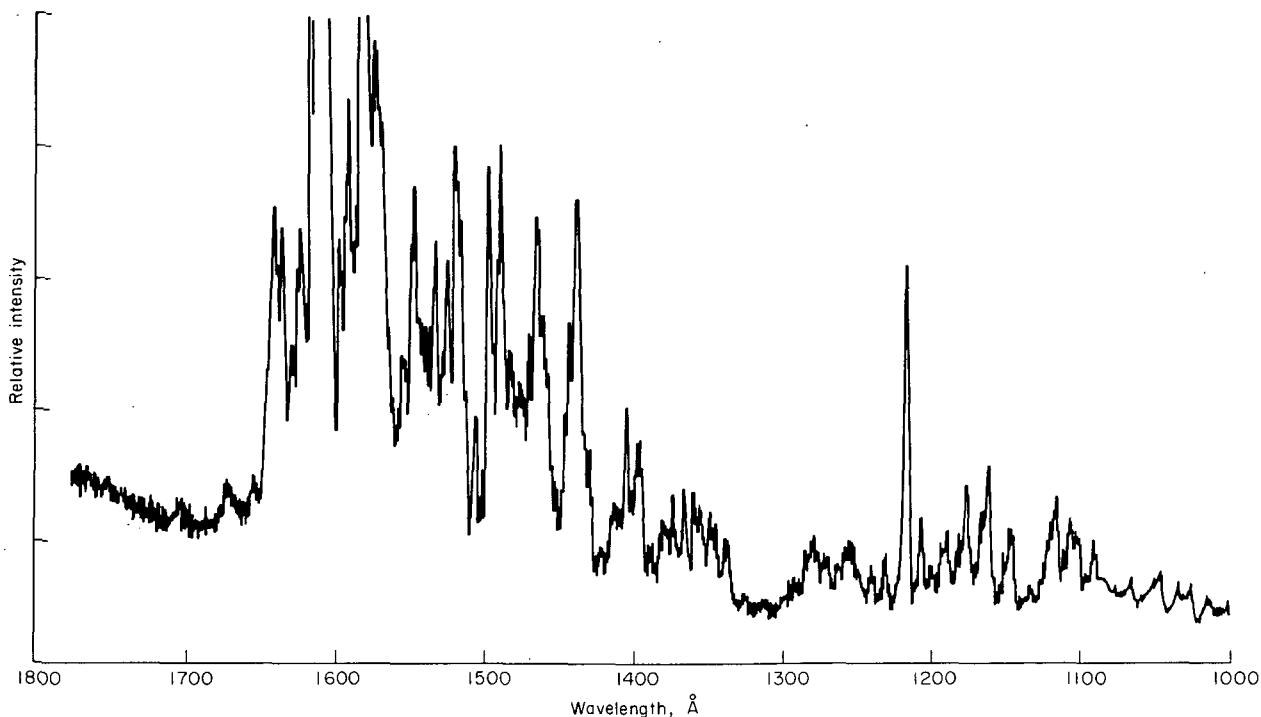


Figure 2. — H<sub>2</sub> emission spectrum as measured by system shown in figure 1.

2537 Å line from this source. A thermocouple detector with a sapphire window was used to calibrate the output of the source-monochromator combination. The thermocouple was calibrated with respect to a quartz iodine lamp that was traceable to NBS standards and accurate to ±15 percent (fig. 4). The detector sensitivity was found from

$$K_{tc} = \frac{i}{I_{tc}} \text{ A/W cm}^2 \quad (14)$$

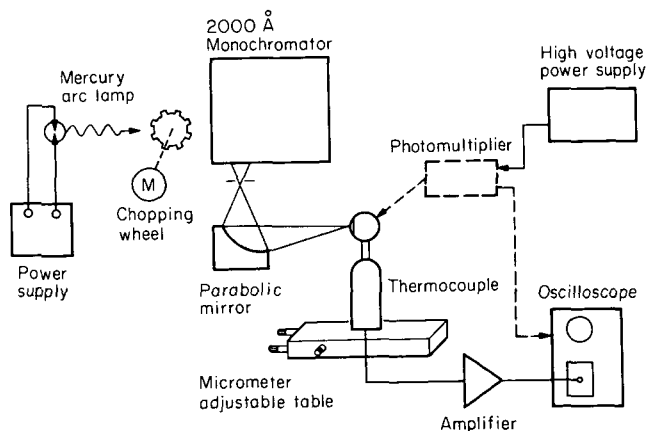


Figure 3. — 2537 Å calibration system.

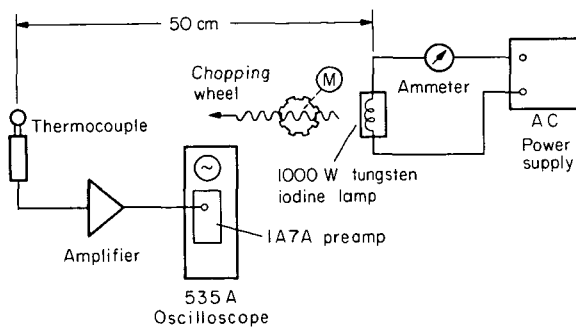


Figure 4. — Setup used to calibrate thermocouple.

where

$$I_{tc} = \int_{\lambda=0}^{\infty} T_{\lambda} R_{\lambda} d\lambda \quad \text{W/cm}^2 \quad (15)$$

and

$R_{\lambda}$  spectral radiant intensity of the lamp,  $\text{W/cm}^2/\text{\AA}$

$T_{\lambda}$  transmission of sapphire thermocouple window, dimensionless

$I_{tc}$  flux density of light falling on the thermocouple,  $\text{W/cm}^2$

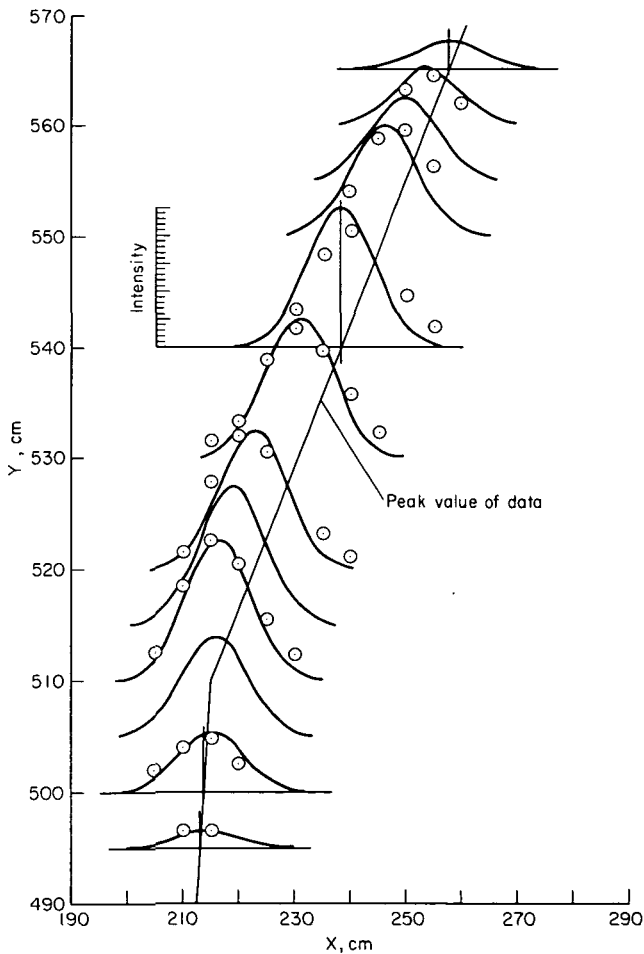


Figure 5. — Topographic display of radiant beam impinging on thermocouple.

Over the wavelength interval of the quartz iodine lamp  $2600 \text{ \AA} < \lambda < 2.6 \mu$ , the spectral response of the thermocouple is assumed to be constant; therefore, this calibration constant can be applied within this interval, and, as is the case here, slightly outside this interval, with confidence.

A further complication arises as a result of the very small size of the thermocouple junction. Even though focusing optics were used to concentrate the radiation emerging from the monochromator onto the thermocouple, and subsequently onto the solar blind photomultiplier, the area of the thermocouple was smaller than the focused beam. The detector was mounted on an X-Y micrometer adjustment table, and a topographic map was made of the variation in intensity within the focal spot (fig. 5). The flux at any point within the focal spot was determined from

$$I_{X,Y} = \frac{i \text{ measured at } X,Y}{T(2537 \text{ \AA})K_{tc}} \quad (16)$$

The total radiant power in the beam was found from

$$P = \int_{X=0}^{\infty} \int_{Y=0}^{\infty} I_{XY} dX dY \quad (17)$$

Once this power was obtained, the solar blind photomultiplier tube was placed in the beam and its cathode sensitivity determined at  $\lambda = 2537 \text{ \AA}$ .

### Calibration at $\lambda = 1470 \text{ \AA}$

To check the results of the first calibration procedure, the cathode sensitivity of the solar blind photomultiplier tube was measured at  $\lambda = 1470 \text{ \AA}$  using a xenon gas discharge lamp, which was provided by the manufacturer of the photomultiplier tube. A similar lamp was used by the manufacturer to establish the calibration curve supplied with the tube. The setup for this calibration is shown in figure 6. This lamp was factory calibrated to an accuracy of  $\pm 30$  percent at a wavelength of  $\lambda = 1470 \text{ \AA}$ , and approximately 90 percent of its total output was at this wavelength. Of the remaining 10 percent, a fair portion is in the visible region, and thus outside of the spectral response of the solar blind photomultiplier tube. Both the lamp output power and beam geometry were provided by the manufacturer (fig. 7(a) and (b)). However, the actual usable solid angle of radiation available from the source was considerably less than that shown in figure 7(b) because (1) the vendor installed a housing around the lamp after it was calibrated at the factory, and (2) limiting or collimating apertures were installed in the experimental apparatus. The resulting half-angle of the cone of radiation from the lamp was  $22.6^\circ$ . The power in that beam was found from

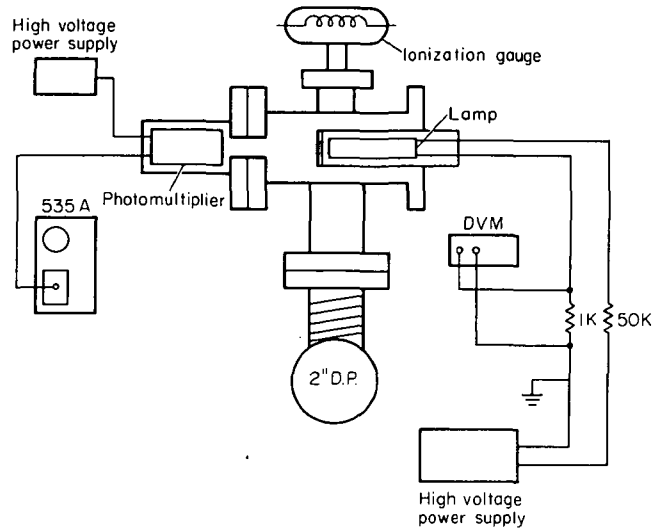


Figure 6. – 1470 Å calibration system.

$$P = P_O \int_0^{2\pi} \int_0^{\theta} \bar{I}_\theta d\omega \quad (18)$$

$$P_O = 2\pi P_O \int_0^{22.6^\circ} \bar{I}_\theta \sin\theta d\theta$$

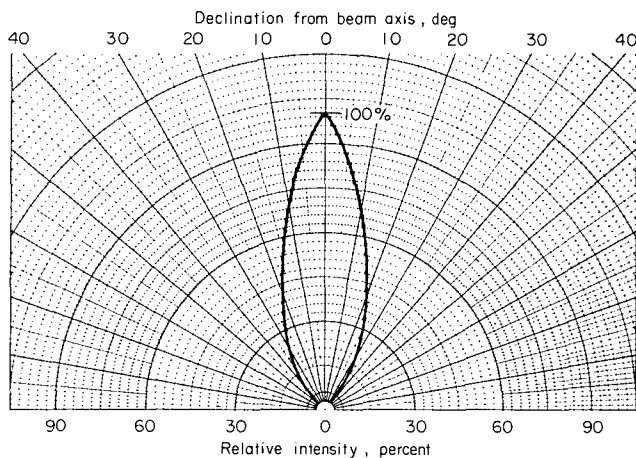
where

$P$  total power in the beam, W

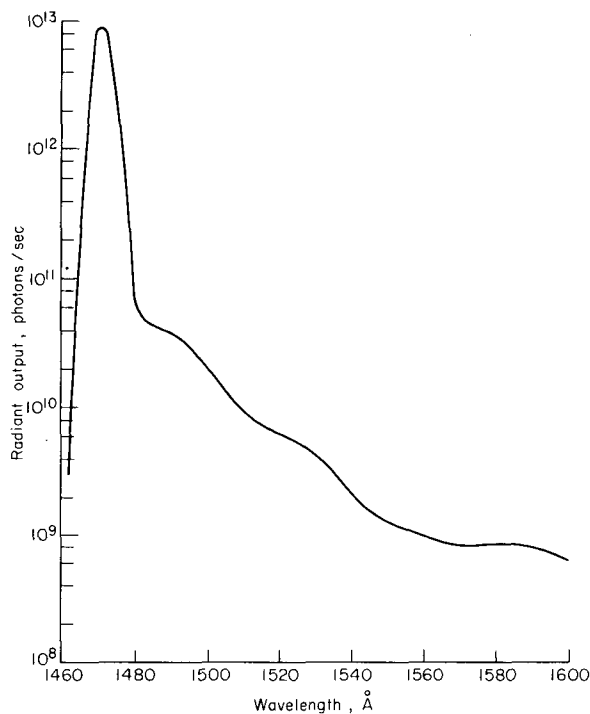
$P_O$  scaling factor, dimensionless

$\bar{I}_\theta$  normalized lamp output/sr (fig. 7(b))

The scaling factor was obtained by taking the vendor's value for the total power from the lamp (in this case  $50 \mu\text{W}$ ) and performing the calculation:



(a) Radial flux distribution for xenon lamp.



(b) Spectral distribution of xenon lamp.

Figure 7. — Characteristics of the xenon lamp.

$$P_O = \frac{50 \mu W}{\int_0^{2\pi} I_\theta d\omega} \quad (19)$$

For the calibration of the solar blind photomultiplier tube at  $\lambda = 1470 \text{ \AA}$  the apparatus was arranged so that all light emerging from the lamp fell on the photomultiplier tube in nearly the same physical location on the photocathode as it would in the actual experiments. The sensitivity of the detectors was found from

$$K_{1470} = \frac{i}{PG} \quad (20)$$

where  $G$  is the gain of external amplifier.

The photomultiplier sensitivity as determined by the above procedures is shown in figure 8.

## DISCUSSION OF RESULTS

The objective of the work was to develop a method for calibrating photosensitive devices in the wavelength region between 1000 and 2000  $\text{\AA}$ . The technique was used to calibrate a particular photomultiplier with spectral response between 1040  $\text{\AA}$  (the short wavelength transmission cutoff

due to its lithium-fluoride window) and 2500 Å (the long wavelength cutoff due to the characteristics of the photocathode material (fig. 8). The error bars on data points were obtained from the following analysis.

### Error Analysis

1. Calibration at  $1100 \text{ \AA} < \lambda < 1600 \text{ \AA}$ .
  - (a) Accuracy of measurements,  $\pm 6$  percent
  - (b) Accuracy of measurement of tube gain,  $\pm 3$  percent
  - (c) Scatter in  $K_{SS}$  data,  $\pm 9.6$  percent
  - (d) Scatter in  $K_{\lambda}$  data,  $\pm 28$  percent

Total uncertainty in spectral response of solar blind detector, approximately  $\pm 40$  percent

2. Calibration at  $\lambda = 2537 \text{ \AA}$ .
  - (a) Accuracy of curve fit, approximately  $\pm 10$  percent
  - (b) Accuracy of thermocouple calibration,  $\pm 15$  percent
  - (c) Data scatter, 5 percent

Total uncertainty of measurement, approximately  $\pm 25$  percent

3. Calibration at  $\lambda = 1470 \text{ \AA}$ .
  - (a) Accuracy of lamp output,  $\pm 30$  percent
  - (b) Accuracy of lamp current measurements,  $< 1$  percent
  - (c) Accuracy of phototube current measurement, 5 percent
  - (d) Data scatter, 5 percent

Total uncertainty of measurements, approximately  $\pm 35$  percent

This list shows that the main source of uncertainty is the scatter in the measurements made at identical conditions when the solar blind detector was calibrated with respect to the secondary

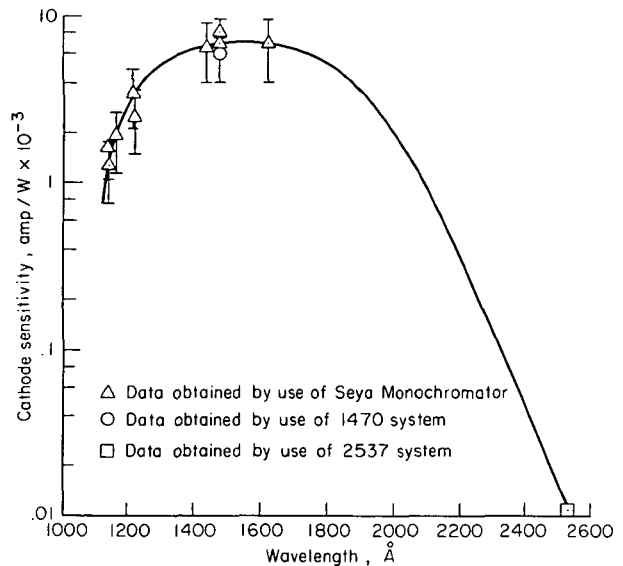


Figure 8. — Cathode spectral response of vacuum ultraviolet phototube.

standards. The light level produced by means of the Seya-Namioka 0.5 m monochromator and Hinteregger lamp was very low. The anode currents from the photomultipliers were typically of the order of  $10^{-11}$  A for the setup used to obtain  $K\lambda$ . The signals were displayed and recorded by strip chart recorders, and high gains (external to the photomultipliers) were required. The data scatter associated with these measurements is large because the systemic noise level in the output was large, although good shielding and "common mode" noise rejection techniques were employed. For the application to which this work was directed, this level of uncertainty ( $\pm 40$  percent) was tolerable. For other applications, however, the level may have to be reduced (e.g., by cooling of amplifiers and detectors and by very careful shielding).

The calibration technique is based on instruments that are available in most research laboratories or may be purchased "off the shelf." Therefore, the calibration would require a minimum of time and effort. The accuracy of calibration actually obtained here is estimated to be  $\pm 40$  percent. Since this number is not based on an error source fundamental to the measurements but rather on experimental system noise, it is probable that a calibration accuracy of  $\pm 10$  percent should be attainable. Furthermore, the same experimental system may be used over a broader spectral range if other noble gases are used in the ionization chamber; Argon, for example, is an absolute standard at wavelengths between 778 and 787 Å.

Ames Research Center  
National Aeronautics and Space Administration  
Moffett Field, Calif. 94035, July 1972

## REFERENCES

1. Samson, James, A. R.: *Techniques of Vacuum Ultraviolet Spectroscopy*. John Wiley & Sons, New York, 1967.
2. Hunter, W. R.: *A Pulsed Light Source for the Extreme Ultraviolet*. Proc. Xth Colloquium Spectroscopicum Internationale, Spartan Books (Washington, D. C.), 1963, pp. 247-261.
3. Namioka, T.: *Theory of the Concave Grating. III. Seya-Namioka Monochromator*. J. Opt. Soc. Amer., vol. 49, no. 10, Oct. 1959, pp. 951-961.
4. Schumacher, B. W.: *The Designing of Dynamic Pressure Stages for High-Pressure/High-Vacuum Systems*. University of Toronto Rep. UTIA 78, AFOSR 88, Aug. 1961.
5. Matsunaga, F. M.; Jackson, R. S.; and Watanabe, K.: *Photoionization Yield and Absorption Coefficient of Xenon in the Region of 860-1022 Å*. J. Quant. Spectrosc. Radiat. Transfer, vol. 5, no. 2, March/April 1965, pp. 329-333.
6. Samson, James A. R.: *Absolute Intensity Measurements in the Vacuum Ultraviolet*. J. Opt. Soc. Amer., vol. 54, no. 1, Jan. 1964, pp. 6-15.
7. Watanabe, K.; and Inn, Edward C. Y.: *Intensity Measurements in the Vacuum Ultraviolet*. J. Opt. Soc. Amer., vol. 43, no. 1, Jan. 1953, pp. 32-35.
8. Schubert, K. E.; and Hudson, R. D.: *A Photoelectric Atlas of the Intense Lines of the Hydrogen Molecular Emission Spectrum from 1025 to 1650 angstrom units at a Resolution of 0.10 angstrom*. Rep. ATN-64(9233)-2, Aerospace Corp., Oct. 4, 1963.



POSTMASTER: If Undeliverable (Section 158  
Postal Manual) Do Not Return

*"The aeronautical and space activities of the United States shall be conducted so as to contribute . . . to the expansion of human knowledge of phenomena in the atmosphere and space. The Administration shall provide for the widest practicable and appropriate dissemination of information concerning its activities and the results thereof."*

— NATIONAL AERONAUTICS AND SPACE ACT OF 1958

## NASA SCIENTIFIC AND TECHNICAL PUBLICATIONS

**TECHNICAL REPORTS:** Scientific and technical information considered important, complete, and a lasting contribution to existing knowledge.

**TECHNICAL NOTES:** Information less broad in scope but nevertheless of importance as a contribution to existing knowledge.

**TECHNICAL MEMORANDUMS:** Information receiving limited distribution because of preliminary data, security classification, or other reasons.

**CONTRACTOR REPORTS:** Scientific and technical information generated under a NASA contract or grant and considered an important contribution to existing knowledge.

**TECHNICAL TRANSLATIONS:** Information published in a foreign language considered to merit NASA distribution in English.

**SPECIAL PUBLICATIONS:** Information derived from or of value to NASA activities. Publications include conference proceedings, monographs, data compilations, handbooks, sourcebooks, and special bibliographies.

**TECHNOLOGY UTILIZATION PUBLICATIONS:** Information on technology used by NASA that may be of particular interest in commercial and other non-aerospace applications. Publications include Tech Briefs, Technology Utilization Reports and Technology Surveys.

*Details on the availability of these publications may be obtained from:*

**SCIENTIFIC AND TECHNICAL INFORMATION OFFICE  
NATIONAL AERONAUTICS AND SPACE ADMINISTRATION  
Washington, D.C. 20546**